Pergamon

Geochimica et Cosmochimica Acta, Vol. 67, No. 14, pp. 2515–2527, 2003

0016-7037/03 $30.00 + .00

doi:10.1016/S0016-7037(03)00078-4

Microscopic reversibility of Sm and Yb sorption onto smectite and kaolinite: Experimental evidence

FRÉDÉRIC COPPIN,* SYLVIE CASTET, GILLES BERGER, and MICHEL LOUBET
University Paul Sabatier/CNRS, LMTG UMR 5563, 38 rue des 36 Ponts, 31400 Toulouse, France

(*Received January* 11, 2002; *accepted in revised form December* 20, 2002)

Abstract—The microscopic reversibility of the sorption of Sm and Yb onto kaolinite and smectite is investigated by introducing an isotopic disequilibrium between the clay and the solution. The experiments are performed at 25°C, in 0.025 or 0.5 M $NaClO_4$ and from pH 4 up to pH 7. The isotopic exchange is monitored as a function of time over a duration of 355 hours. The first stage of the experiment consists of equilibrating the clays with a natural or spiked lanthanide solution. The second stage consists of interchanging the solutions between twin phials (same clay, pH and ionic strength, but with different lanthanide isotopic compositions). The isotopic composition and concentration of aqueous lanthanides are analysed by ICP-MS. The results are as follows: (1) the lanthanide isotopic composition of the solution is rapidly modified and stabilised within 24 h; (2) the isotopic exchange between the solid and the solution is not always complete; (3) the degree of microscopic reversibility (isotopic exchange) decreases with increasing pH. These results are explained by the fact that exchange is easier for lanthanides linked to the surface as outer-sphere complexes (physical sorption), which predominate at low pH, than for atoms sorbed as inner-sphere complexes (chemical sorption) which predominate at high pH. The contrasted kinetics observed for the different kind of sites provide additional constraints for the modeling of migration processes in natural systems. *Copyright © 2003 Elsevier Science Ltd*

1. INTRODUCTION

The increasing number of environmental studies on the behaviour of lanthanides (or rare earth elements, REE) in natural solutions has provided ample evidence that the reactions at the solid/solution interface are of great importance in controlling the REE concentrations in rivers, groundwaters and sea water (Goldstein and Jacobsen, 1988; Sholkovitz, 1995; Sholkovitz et al., 1999). As a consequence, several experimental studies have focused on the quantification of REE adsorption. These studies are often conducted with simple minerals, such as Fe, Mn, Si or Al oxides or oxy-hydroxides (De Carlo et al., 1998; Koeppenkastrop and De Carlo, 1992; Kosmulski, 1997; Marmier et al., 1993; Wang et al., 2000). In spite of the common presence of clay minerals in natural solutions (as suspended or bed-load material), only a few authors have investigated REE sorption onto these minerals (Aja, 1998; Kulik et al., 2000; Laufer et al., 1984; Maza-Rodriguez et al., 1992; Nagasaki et al., 1997). However, the recent paper by Coppin et al. (2002) provides a full and coherent dataset involving sorption onto kaolinite and a Na-montmorillonite, as a function of pH, ionic strength and atomic number of the lanthanide. These data, supplemented by the spectroscopic study of Stumpf et al. (2001), provide evidence for two sorption mechanisms: surface complexation by amphoteric sites at the edges of the clay particles, and exchange with the compensating interlayer cations. The former involves inner-sphere complexes, leads to fractionation of the REE pattern and is strongly pH-dependent. The latter involves outer-sphere complexes, does not lead to fractionation of the REE pattern and depends on the cationic exchange capacity of the clay, not on pH.

This mechanistic interpretation, which distinguishes two radically different reactions, suggests that the kinetics of these reactions could also be very different. In particular, the reversibility of the two reactions is not well documented. Previous studies have examined the reversibility of metal sorption onto clays and have yielded contrasted conclusions. Some studies, such as Turner et al. (1998) and Undabeytia et al. (1998) on the sorption of Np and Cd onto a montmorillonite, respectively, conclude that the sorption process is a fully reversible reaction. On the other hand, other studies including Bonnot-Courtois and Jaffrezic-Renault (1982), failed to observe any reversibility of the lanthanide sorption onto either montmorillonite or illite. Other experimentators observed hysteresis-type behaviour between the adsorption and the desorption reactions and have attributed the irreversible character of the sorption to particular sites within the minerals (Miller et al., 1982). But the results of adsorption-desorption experimental cycles can be difficult to interpret given the chemical perturbations generated by the cycles (see, Undabeytia et al. (1998) for example).

In the present study, we focus on another aspect of the kinetics of REE sorption onto clays, that is, the elementary exchange occurring at the microscopic scale when the system is in macroscopic equilibrium. According to the concept of microscopic reversibility, forward and backward elementary reactions occur simultaneously and compensate at equilibrium. When applied to sorption processes, this implies that desorption and adsorption reactions affect the solid/solution interface, even when the chemical composition of the solution remains constant with time. Basing our work on the experimental approach of Comans et al. (1991), we investigated the microscopic reversibility of lanthanide sorption by monitoring the behaviour of isotope tracers (^{149}Sm and ^{172}Yb) after attaining chemical equilibrium in clay suspensions. As a continuation of

* Author to whom correspondence should be addressed (berger@lmtg.ups-tlse.fr).

Table 1. Sm and Yb concentrations and isotopic compositions in the two REE stock solutions.

	Concentration (ppb)		Isotopic abundance (% of total element)													
Solution	Sm	Yb	^{144}Sm	^{147}Sm	^{148}Sm	^{149}Sm	^{150}Sm	^{152}Sm	^{154}Sm	^{168}Yb	^{170}Yb	^{171}Yb	^{172}Yb	^{173}Yb	^{174}Yb	^{176}Yb
Natural	50726	54817	2.8	14.0	10.7	13.7	7.4	27.5	23.8	0.2	3.0	14.0	21.6	16.1	32.0	13.1
Spiked	52342	52163	0.0	0.2	0.8	96.2	1.5	1.0	0.2	0.0	0.0	1.3	95.9	1.5	1.1	0.2

Coppin et al. (2002), we carried out experiments at 25°C with suspensions of kaolinite and Na-montmorillonite in 0.5 and 0.025 mol/L $NaClO_4$ solutions at various pH values. The originality of our approach consists of interchanging the fluids of twin experiments conducted using natural or spiked Sm and Yb salts. When the pH and the lanthanide concentrations are identical in the twin experiments, this procedure allows us to introduce an isotopic disequilibrium between the aqueous and sorbed lanthanides, without perturbing the chemical equilibrium of the system.

2. EXPERIMENTAL SETUP

We used the following procedure to identify the degree of progress of the microscopic reversibility:

1. an equilibrium between clays and REE solution is first attained through classical adsorption experiments at different pH and ionic strengths;
2. the isotopic composition of the solution is then modified without changing its global concentration to maintain solid/solution chemical equilibrium.

The evolution of the REE isotopic composition of the solution is monitored as a function of time, to evaluate the isotopic exchange of REE between species sorbed onto the solid and ions in solution.

2.1. Lanthanide Stock Solutions

The stock solutions were prepared in 20-mL polypropylene bottles using a $2\%_w HNO_3$ solution made with deionised water (Milli-Q Reagent Water System from, Millipore Corp.) with a resistivity higher than 18 $M\Omega \cdot cm^{-1}$ and bi-distilled nitric acid.

Two stock solutions containing Sm and Yb were prepared: one with a lanthanide isotopic composition near the naturally occurring value (called "Natural" in the following text) and the other with a non-natural isotopic composition (called "Spiked" in the following text). This latter was obtained from spiked metals (Russian origin, certificates N° 91 and N° 667 for Sm and Yb, respectively) dissolved with concentrated and pure HCl, which was then diluted. The "Natural" solution was made from solid REE oxides (Johnson Mattey products) dissolved with HCl and then diluted. The final Sm and Yb concentrations and isotopic compositions of the two stock solutions are reported in Table 1.

2.2. Starting Clays and Suspensions

The clays used in this work are the same as those used in a prior study, which dealt with the sorption of lanthanides on smectite and kaolinite (Coppin et al., 2002). Two types of clays were used: a kaolinite and a dioctahedral smectite. The kaolinite is a well-crystallised fine-grained kaolinite (≤ 2 μm) from St. Austell (UK). The smectite corresponds to the < 0.2 μm fraction of the Ceca bentonite separated by sedimentation techniques (Day, 1965) and then saturated with Na. The specific surface areas, measured by N_2 adsorption (BET method), are 12 m^2/g for the kaolinite and 32 m^2/g for the smectite. The measured cation exchange capacities (CEC) of the initial clays were 3.7 meq/100g for kaolinite and 75 meq/100g for smectite, using the method proposed by Meier and Kahr (1999). A more detailed description of the kaolinite and smectite used in our experiments can be found in Bauer and Berger (1998) and Bauer and Velde (1999).

Four clay suspensions were prepared in volumetric flasks by mixing 250 mg of each mineral (kaolinite or smectite) with 250 mL of a 0.025 mol/L or 0.5 mol/L analytical grade $NaClO_4$ solution (Prolabo, RP Normapur), used as background electrolyte to buffer the ionic strength of the solutions. These suspensions were shaken continuously for 48h with a magnetic stirrer, to reach steady Si and Al concentrations in solution according to Coppin et al. (2002). Under these experimental conditions, no secondary solid phases were formed as checked by X-ray diffraction (XRD) (see details in Coppin et al., 2002).

2.3. Analytical Method

The isotopic compositions and concentrations of aqueous Sm and Yb were analysed by Inductively Coupled Plasma Mass Spectrometry (ICP-MS, Perkin-Elmer Elan-6000). For each element, the abundances of the seven isotopes were determined. The precision is better than 5% for the measurable isotopes, which are the only ones used in the calculations. We used a "Natural" solution containing 10 ppb of Sm and Yb as an external standard and ^{115}In as an internal standard, to correct for possible instrumental drift. The isobaric interference corrections applied are given in Aries et al. (2000).

2.4. Experimental Procedure

The microscopic reversibility of the adsorption process was studied at 25°C, at two ionic strengths (0.025M and 0.5M), and as a function of pH and time. The experiments were carried out in two successive stages described below and diagrammatically represented on Figure 1.

2.4.1. First stage: sorption experiments

In the first part of the present study, Sm and Yb are sorbed onto the clays at different pH and ionic strengths. The experi-

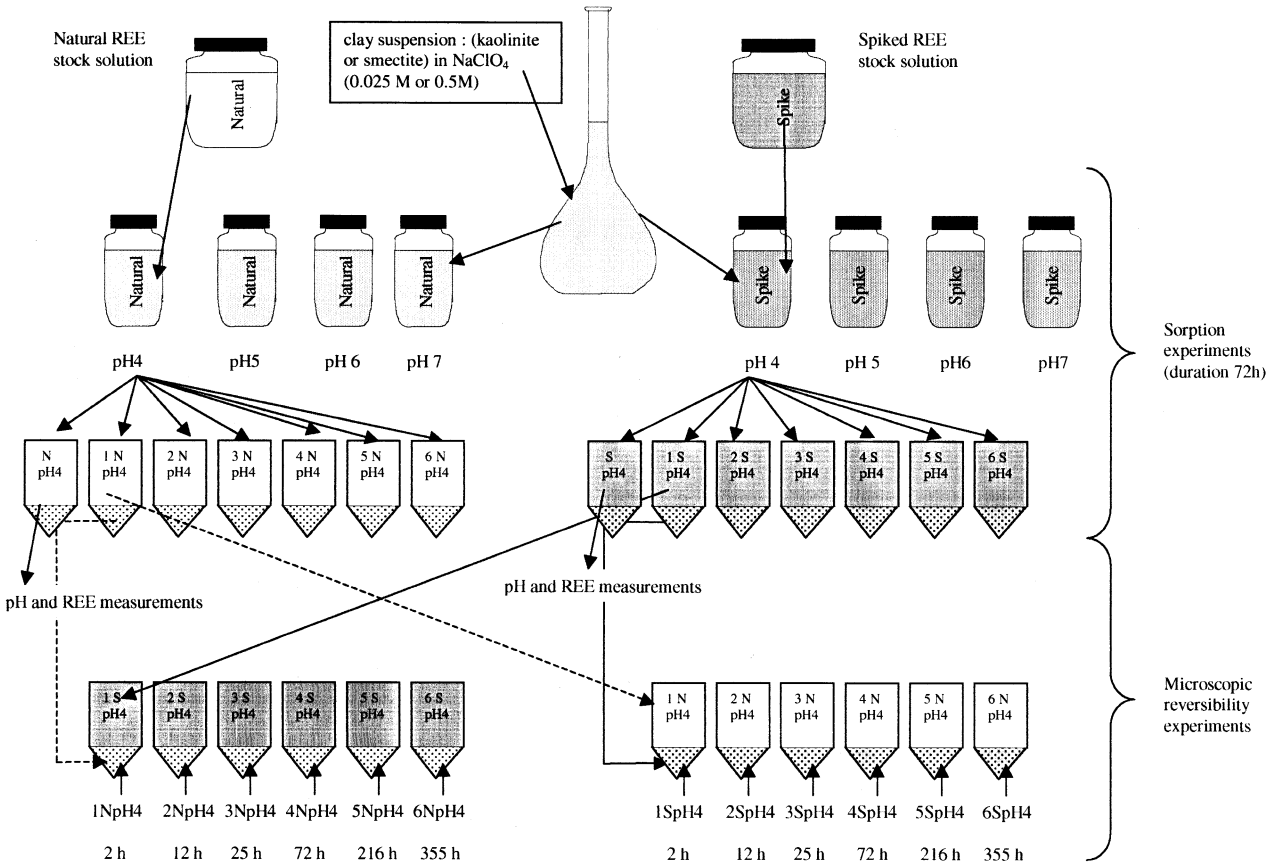

Fig. 1. Schematic diagram of the experimental procedure.

ments are carried out following the procedure developed in Coppin et al. (2002) with the objective to reach a steady state where the Sm and Yb contents in the solid and the solution are in equilibrium.

To perform these experiments, 20 mL of each clay suspension are introduced into a polypropylene bottle into which are added 40 μL of the stock lanthanide solution ("Natural" or "Spiked") to obtain ~105 ppb of each lanthanide in the samples. We assume that the clay suspension samplings are homogeneous. The pH is adjusted at the desired value, nearly 4, 5, 6 or 7 using a NaOH solution (Prolabo, RP Normapur). In this manner, sixteen samples are obtained for each mineral: "Natural" or "Spiked" lanthanides solutions, at two ionic strengths and four pH values. As in our previous study (Coppin et al., 2002), these samples are shaken for 72 h to avoid sedimentation and to ensure that most of sites are accessible. This duration is long enough to reach steady lanthanide concentrations in solution. After this reaction time, seven aliquots of 2 mL are taken from each suspension and centrifuged (3500 rpm for 40 min) to separate the solid from the solution. For one of these aliquots, the supernatant is divided in two fractions, one for pH measurement, while the other is diluted and acidified (2% HNO_3) for Sm and Yb ICP-MS analysis. The remaining six aliquots are reserved for the subsequent experiments. The absence of significant REE adsorption by the containers was verified by specific treatment of the containers after the run and analysis of the recollected solution (see Coppin et al., 2002).

2.4.2. *Second stage: microscopic reversibility experiments*

After centrifugation, the supernatants of the six remaining aliquots are interchanged between two twin phials, i.e., phials with the same clay, the same ionic strength, the same pH, but one containing the "Natural" lanthanide solution and the other the "Spiked" solution. Then, the phials are shaken again to put the clay back into suspension. In that way, the isotopic compositions of lanthanides between the solid and the solution are modified but, in the ideal case, not the equilibrium concentrations of the lanthanides (see section 2.4.3). Thus, we obtain two sets of phials: a first set with "Spiked" solid and "Natural" solution and the other with "Natural" solid and "Spiked" solution. For each mineral, at each ionic strength and pH, we thus obtain twelve new suspensions. They are centrifuged (3500 rpm for 40 min) after respectively 2, 12, 25, 72, 216 and 355 h of reaction time. The supernatant is then divided in two fractions, one for pH measurement, while the other is diluted and acidified (2% HNO_3) for further Sm and Yb ICP-MS analysis. By this procedure, we can monitor the variations of isotopic composition and concentrations of aqueous Sm and Yb as a function of time.

2.4.3. *Taking account of artefacts due to the experimental procedure*

In the ideal case, the pH and the lanthanide concentrations of the solution at the end of twin sorption experiments (same

Table 2. pH, concentrations, Log K_D and REE isotopic abundances (^{149}Sm and ^{172}Yb) at the end of the sorption experiments: example of smectite, at I = 0.5M.

		Sm		Yb		Log K_D ($mL.g^{-1}$)		Isotopic abundance (% of total element)	
Solution	pH (± 0.05)	$C_{initial}$ (ppb)	C_{final} (ppb)	$C_{initial}$ (ppb)	C_{final} (ppb)	Sm	Yb	^{149}Sm	^{172}Yb
Natural	4.67	101	87	110	96	2.2	2.2	13.8	21.5
	5.69	101	69	110	62	2.7	2.9	13.7	21.6
	6.30	101	44	110	19	3.1	3.7	13.8	21.3
	6.62	101	10	110	3	4.0	4.5	13.8	21.4
Spiked	4.37	104	96	104	98	1.9	1.7	95.7	95.7
	5.76	104	78	104	70	2.5	2.7	95.8	95.6
	6.37	104	42	104	18	3.2	3.7	95.4	95.7
	6.59	104	11	104	3	3.9	4.5	94.2	95.7

starting clay, pH and ionic strength, but one "Spiked" and the other "Natural") should be identical. This is evidently not quite the case. In the interpretation of the data given here, we take into account the observed variations from the ideal case and their possible consequences on the results.

As an example, Table 2 reports the pH measured for the smectite at high ionic strength at the end of the first stage for twin sorption experiments. The largest pH difference between the twin phials before the solution changeover is less than 0.3 pH unit. A similar order of pH variation is observed in the other experiments. In Figure 2, we report the pH measured at the end of microscopic reversibility experiments, performed with the "spiked" smectite and the "Natural" REE solution at I=0.025M, as a function of time. Similar results have been obtained with other studied systems. From this plot, we can see that the most important pH difference (± 0.3 U) between experiments is observed in the first 25 h, then the pH stabilises to within ± 0.15 U. The pH difference observed at the end of the sorption experiment between the twin phials is included in this narrow bracket. Even if these variations are weak, they can eventually drive a change in REE aqueous concentration.

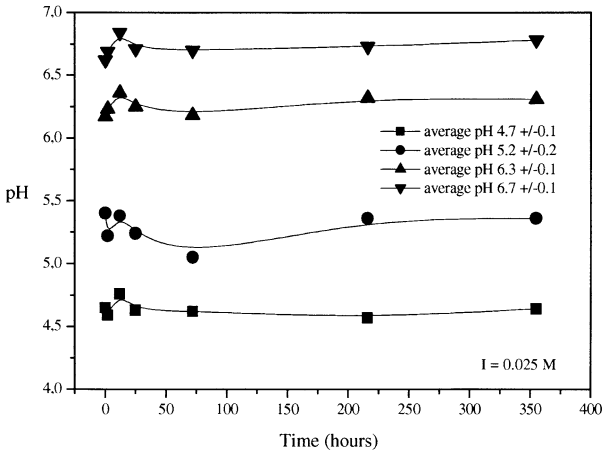

Fig. 2. pH measured in solution at the end of microscopic reversibility experiments versus reaction time. Example of data obtained with smectite, at low ionic strength, for Spiked solid and Natural solution initial conditions (the curves correspond to a smoothed interpolation of the data).

This phenomena can explain the observed difference in REE concentrations measured in solutions, at the end of sorption experiments between the twin phials, i.e.: of the order of 10% or lower for most cases, but up to 50% in some cases when the REE content in solution is low (≤5 ppb). These differences can lead to chemical solid/solution REE exchange when the twin solutions are interchanged. Indeed, if the lanthanide concentration of the new solution is higher than the replaced one, the solid will adsorb lanthanides from the second solution to reach a new equilibrium. On the other hand, if the lanthanide concentration of the new solution is lower than the replaced solution, the solid will release some lanthanides to reach equilibrium. Under this condition, re-equilibration will affect the isotopic composition of the second solution. However, this process should not be confused with an isotopic exchange resulting from microscopic reversibility. Knowing the increase in aqueous REE concentrations and the isotopic composition of the released REE, this chemical re-equilibration can be estimated and taken into account in the interpretation of the results by including a coefficient (named *b*) in our isotopic calculations (see section 4).

Finally, another limitation of our experimental procedure is the persistence of a small fraction of the first solution - linked to the clay - which remains after centrifugation and during withdrawal of the solution. This residual interstitial solution can affect the isotopic composition of the second solution. In this case, the isotopic composition of this residual liquid film is assumed to be the same as that sorbed onto the solid phase and its REE concentration is identical to that of the withdrawn solution. The mass of this interstitial liquid film was determined by weighing the container at each step of the procedure, to apply appropriate corrections in the calculation of isotopic exchange (see section 4). On average, the residual liquid represents ~0.7% by weight of the solution.

3. RESULTS

As already mentioned, seven isotopes of the lanthanides Sm and Yb were analysed throughout this study (Table 1). For each of the elements, the set of measured isotopes show the same behaviour. Because of this, and for reasons of clarity, we selected two specific isotopes to study the experimental results: ^{149}Sm and ^{172}Yb. The reasons for this choice are: i) these isotopes are enough abundant for each element (>10%) to be

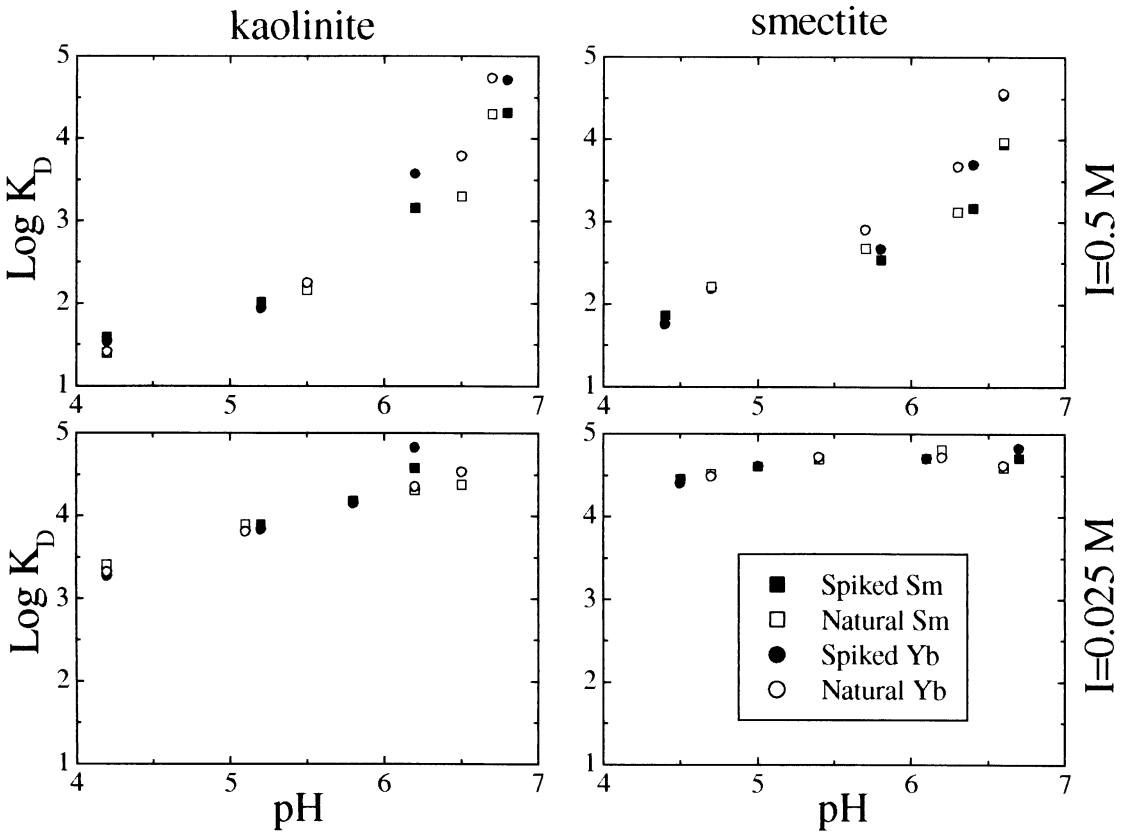

Fig. 3. Logarithm of calculated K_D for Sm and Yb as a function of pH, ionic strength and nature of clay. In the legend, spike corresponds to sorption experiments realized with the spiked solution of rare earth elements and natural with the natural one.

analysed with a good precision and ii) the proportion of each isotope in the "Natural" and "Spiked" solutions are sufficiently different to prevent misinterpretation of the results (Table 1).

3.1. Sorption Experiments

Since the quantification of the REE sorption onto clays is presented elsewhere, we present here only the major results and refer the reader to our previous work (Coppin et al., 2002) for more data on this topic. As an example, Table 2 presents the concentrations and isotopic abundances measured in solution for the experiments with smectite at high ionic strength (0.5 mol/L) as a function of pH. The logarithms of the corresponding distribution coefficients, K_D, are also reported. This parameter is calculated from the following equation:

$$K_D\ (\text{mL/g}) = \frac{(C_{\text{initial}} - C_{\text{final}})}{C_{\text{final}}} * \frac{V}{M} \quad (1)$$

where C_{initial} and C_{final} are the aqueous concentrations (μg/L) of lanthanides at the beginning and end of the experiment, V is the volume of the solution (mL) and M is the mass of solid (g).

For both Sm and Yb, the K_D values determined in the present study are in agreement with those obtained in our previous work (Coppin et al., 2002). Figure 3 shows the log K_D obtained for sorption experiments of Sm and Yb as a function of pH, ionic strength and nature of clay. More generally, we observe the same REE behaviour and the same range of K_D values as previously demonstrated. At high ionic strength (I=0.5 mol/L), for both clays, the percentage of sorbed lanthanides is strongly pH dependent and increases from 10% (log $K_D \approx 1.5$) to nearly 95% (log $K_D \approx 4.5$) over a narrow pH range (from 6 to 7). At low ionic strength (I=0.025 mol/L), and for both clays, the quantity of sorbed REE at pH 4–7 is higher than at I=0.5 mol/L (log $K_D \approx$3.5–4.5). Moreover, for smectite at low ionic strength, the percentage of sorbed REE is almost pH independent over the studied pH range (log $K_D \approx 4.5$). At 0.5 mol/L, both minerals exhibit the same pH-dependent REE sorption behaviour. At this high ionic strength the permanent charge (CEC) is compensated by the background electrolyte and the data monitor only the REE chemisorption on amphoteric sites at the edges of particles. At 0.025 mol/L, the measured K_D are more influenced by the CEC of the minerals and exhibit high values even at low pH (Coppin et al., 2002). Finally, we can see from Table 2 that the REE isotopic abundances are not significantly modified during the sorption process. As an example, Table 2 gives the concentrations and isotopic abundances measured in the solution at the end of the sorption experiment for smectite, at high ionic strength (0.5 mol/L). Only the "Spiked" solution shows a slight decrease in the ^{149}Sm content. According to our previous study (Coppin et al., 2002) this behaviour may be attributed to the release into solution of a small amount of lanthanides from the initial clay, due to a slight dissolution

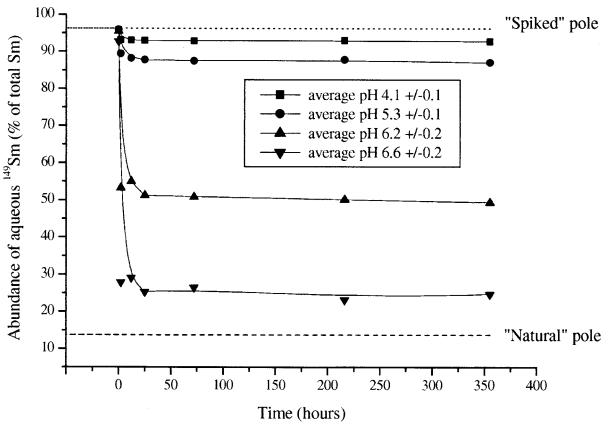

Fig. 4. ^{149}Sm isotopic abundance measured in solution versus reaction time (filled symbols). Example of kaolinite, at high ionic strength, for Natural solid and Spiked solution initial conditions. The two dashed lines represent the pure initial end-members (the curves correspond to a smoothed interpolation of the data).

of the mineral (1.3 ppb of Sm at pH about 4 for experiments conducted with 7g/L of smectite). Nevertheless, such a slight isotopic variation of the solution does not modify the following interpretations since these are based on the isotopic abundances measured at the end of the sorption experiments.

3.2. Kinetic of Isotopic Exchange

During the second stage of the experimental procedure, the isotopic composition of the solutions are monitored as a function of time (2, 12, 25, 72, 216 and 355 h, respectively). As an example, Figure 4 shows the aqueous ^{149}Sm isotopic abundance (percentage of total Sm), as a function of time and at different pH, measured in the run conducted with "Natural" kaolinite and "Spiked" solution, at high ionic strength. The ^{149}Sm abundances of the starting stock solutions are also reported on this diagram, and identified as "Spiked" and "Natural" end-members. Irrespective of the pH of the experiment, the abundance of aqueous ^{149}Sm decreases very rapidly (a few hours) to reach a plateau from 25 to 355 h of reaction time. Such rapid equilibration of the isotopic exchange has also been reported by Comans et al. (1991) in a study of Cs sorption on illite. On the other hand, the intensity of the observed decrease is pH dependent and related to the percentage of sorbed REEs. The more basic the pH, the greater the quantity of sorbed REEs, so they will exert a greater influence on the isotopic composition of the solution. The same occurs in the other experiments in which the range of variation of the isotopic abundance in solution is a function of the percentage of sorbed REEs in each experiment (see section 3.1 and Tables 3 and 4).

3.3. Isotopic Composition of the Solution at the End of the Microscopic Reversibility Experiments

Because the system reached an equilibrium or steady state very rapidly, we decided to use only the data obtained at 355 h reaction time in discussion of the results. The corresponding abundances of the aqueous ^{149}Sm and ^{172}Yb are reported on Figure 5 (solid symbols) as a function of pH, ionic strength and nature of the clay. The data were obtained from experiments using "Natural" solids and "Spiked" solutions as starting conditions. The initial REE isotopic composition of the solid and solution end-members are indicated on Figure 5 by the two dashed-dotted lines which are labelled NP and SP for "Natural" and "Spiked" end-members, respectively.

Except in the case of smectite at low ionic strength, the fractions of both ^{149}Sm and ^{172}Yb in solution decrease with increasing pH. At high ionic strength and with pH $\approx$ 7, isotopic abundances decrease from a value close to the "Spike" composition ($\sim$90%) at pH $\approx$ 4, to reach 25% or 40%, depending on the mineral. At low ionic strength, the results differ from one mineral to another. With kaolinite, the isotopic abundance decreases from nearly 45% at pH $\approx$ 4, to nearly 20% at pH $\approx$ 7. With smectite, the isotopes show a special type of behaviour: their abundances are very close to the "Natural" end-member composition over the entire investigated pH range.

4. DISCUSSION

To determine the fraction of lanthanide isotope that has exchanged between the solution and the clay, we must first evaluate the isotopic compositions expected in the solution at the end of each experiment for different percentages of exchangeable lanthanides. This can be done using simple mixing equations.

The isotopic composition of a product formed by the mixing of two end-members denoted 1 and 2 can be written as:

$$A_{mixing} = \frac{A_1N_1 + A_2N_2}{N_1 + N_2} \quad (2)$$

Where

A_{mixing} is the abundance of the considered isotope in the mixed product,
A_i is the abundance of the considered isotope in end-member i,
N_i is the number of atoms of the considered element in end-member i.

Since each element is composed of a certain number of isotopes, we define abundance here as the percentage of the considered isotope in the element in question.

Here, the two end-members correspond to the solid and the solution at the beginning of the experiments.

In a very simple initial approach, Eqn. 2 is applied to compute the ^{152}Sm/^{149}Sm composition of the final solution resulting from: (a) total mixing of the REE from the solid and the solution, thus assuming a total REE re-equilibration between the two phases, (b) partial exchange involving 10% of the cations sorbed onto the solid. The computed results are reported on Figure 6 as a function of the percentage of sorbed REE on the solid (100 and 10% curves, respectively). On the same figure, these results are compared with the experimental data (squares) obtained with the two clays at the two ionic strengths, for "Spiked" solution and "Natural" solid initial conditions, after 355 h reaction time. From Figure 6**,** we can see that the overall experimental results do not fit with the computed data corresponding to total equilibrium between the solid and the solution (100% curve). However, this curve cannot be taken as a precise evolution of the REE isotopic composition in solution because the different experimental artefacts are not

Table 3. Percentage of element sorbed onto the solid as a function of pH. Summary table of results obtained for microscopic reversibility experiments at 355 h, for the two ionic strengths, the two clays, for ^{149}Sm and ^{172}Yb and for Natural solid/Spiked solution starting conditions. The uncertainties on % are calculated from analytical standard deviations.

		Kaolinite I = 0.025 M				Kaolinite I = 0.5 M				Smectite I = 0.025M				Smectite I = 0.5M			
Natural Ln in solid and Spiked Ln in solution	pH (± 0.05)	4.17	5.25	6.12	6.48	4.08	5.40	6.27	6.44	4.57	5.40	6.31	6.77	4.64	5.95	6.34	6.47
	% Sm sorbed	72	89	96	96	2	13	66	96	97	98	98	98	14	32	57	90
	[Sm]initial (ppb)	32	11	6	3	105	98	45	5	3	2	2	2	97	78	42	11
	[Sm]final (ppb)	33	9	6	5	105	94	45	12	2	2	3	3	98	63	33	16
	^{149}Sm (% total Sm) measured	42.3 (± 0.3)	24.2 (± 0.6)	19.7 (± 0.4)	16.4 (± 0.6)	92.8 (± 0.1)	87.1 (± 0.2)	49.4 (± 0.5)	24.7 (± 0.4)	15.2 (± 0.6)	15.5 (± 1.0)	16.7 (± 0.4)	16.4 (± 0.7)	88.1 (± 0.1)	73.7 (± 0.3)	50.8 (± 0.3)	39.9 (± 0.4)
	^{149}Sm (% total Sm) calculated (Eqn 3)	91.2	94.6	84.1	46.0	94.5	95.6	95.2	46.3	89.9	85.7	61.5	71.2	94.2	95.4	95.1	69.3
	^{149}Sm (% total Sm) calculated (Eqn 4)	38.9	22.6	17.9	14.4	92.8	85.9	46.1	17.0	15.6	14.3	14.9	15.0	84.7	71.4	48.0	22.5
	% Yb sorbed	67	87	96	97	1	15	86	98	97	98	98	98	13	44	83	98
	[Yb]initial (ppb)	37	14	7	2	105	98	23	2	4	2	2	2	98	70	17	3
	[Yb]final (ppb)	39	12	7	4	105	95	25	6	3	3	3	2	100	45	14	5
	^{172}Yb (% total Yb) measured	49.3 (± 0.5)	32.6 (± 0.5)	27.4 (± 0.4)	24.0 (± 0.4)	93.2 (± 0.1)	85.8 (± 0.2)	37.9 (± 0.4)	25.8 (± 0.7)	24.1 (± 0.5)	24.3 (± 0.5)	26.0 (± 0.5)	26.0 (± 1.2)	88.8 (± 0.1)	67.4 (± 0.2)	37.1 (± 0.3)	32.0 (± 0.7)
	^{172}Yb (% total Yb) calculated (Eqn 3)	90.7	95.2	93.5	52.8	94.2	95.2	89.2	45.0	94.6	82.7	71.6	69.8	94.0	95.3	95.3	64.4
	^{172}Yb (% total Yb) calculated (Eqn 4)	46.7	30.9	26.5	22.9	93.2	84.7	36.0	22.2	23.9	23.1	22.7	22.8	85.8	65.2	33.3	23.3

Table 4. Percentage of element sorbed onto the solid as a function of pH. Summary table of results obtained for microscopic reversibility experiments at 355 h, for the two ionic strengths, the two clays, for ^{149}Sm and ^{172}Yb and for Spiked solid/Natural solution starting conditions. The uncertainties on % are calculated from analytical standard deviations.

		Kaolinite I = 0.025 M				Kaolinite I = 0.5 M				Smectite I = 0.025M				Smectite I = 0.5M			
Spiked Ln in solid and Natural Ln in solution	pH (± 0.05)	4.17	5.33	6.39	6.44	3.91	5.45	6.52	6.64	4.64	5.36	6.31	6.78	4.70	5.89	6.47	6.61
	% Sm sorbed	68	89	94	98	4	9	58	95	96	98	98	98	7	25	60	89
	[Sm]initial (ppb)	23	11	5	4	101	90	35	5	3	2	2	2	87	69	44	10
	[Sm]final (ppb)	29	9	5	5	100	83	21	6	2	2	3	3	85	53	26	8
	^{149}Sm (% total Sm) measured	73.1 (± 0.3)	87.6 (± 0.2)	91.7 (± 0.1)	91.4 (± 0.2)	16.9 (± 0.3)	21.7 (± 0.2)	61.9 (± 0.3)	85.3 (± 0.2)	85.6 (± 0.4)	84.5 (± 0.3)	81.1 (± 0.4)	85.0 (± 0.2)	21.3 (± 0.2)	35.9 (± 0.3)	56.3 (± 0.6)	74.8 (± 0.4)
	^{149}Sm (% total Sm) calculated (Eqn 3)	18.5	13.7	27.1	30.4	14.0	14.1	14.1	32.8	13.2	34.9	43.5	25.5	14.2	14.1	14.2	14.2
	^{149}Sm (% total Sm) calculated (Eqn 4)	71.4	85.7	89.9	87.3	17.3	22.4	66.2	89.2	87.8	90.5	92.7	89.8	20.4	36.2	61.6	86.3
	% Yb sorbed	65	87	93	98	3	8	79	98	96	98	98	98	5	32	83	97
	[Yb]initial (ppb)	35	14	5	3	109	94	15	2	4	2	2	3	95	61	19	3
	[Yb]final (ppb)	34	12	5	5	107	82	9	3	2	3	3	3	93	40	10	3
	^{172}Yb (% total Yb) measured	71.5 (± 0.2)	86.3 (± 0.2)	91.7 (± 0.1)	92.5 (± 0.1)	23.8 (± 0.4)	29.3 (± 0.4)	81.0 (± 0.3)	91.2 (± 0.2)	93.5 (± 0.1)	93.5 (± 0.1)	86.5 (± 0.4)	86.2 (± 0.4)	27.4 (± 0.2)	48.0 (± 0.4)	75.9 (± 0.5)	87.1 (± 0.3)
	^{172}Yb (% total Yb) calculated (Eqn 3)	21.8	21.7	22.2	52.9	22.1	22.1	22.2	48.3	21.6	37.8	33.5	19.8	21.9	22.0	21.6	34.1
	^{172}Yb (% total Yb) calculated (Eqn 4)	70.6	85.9	92.2	93.8	24.2	28.3	83.9	93.9	92.5	94.3	94.0	93.7	25.7	47.7	81.9	93.5

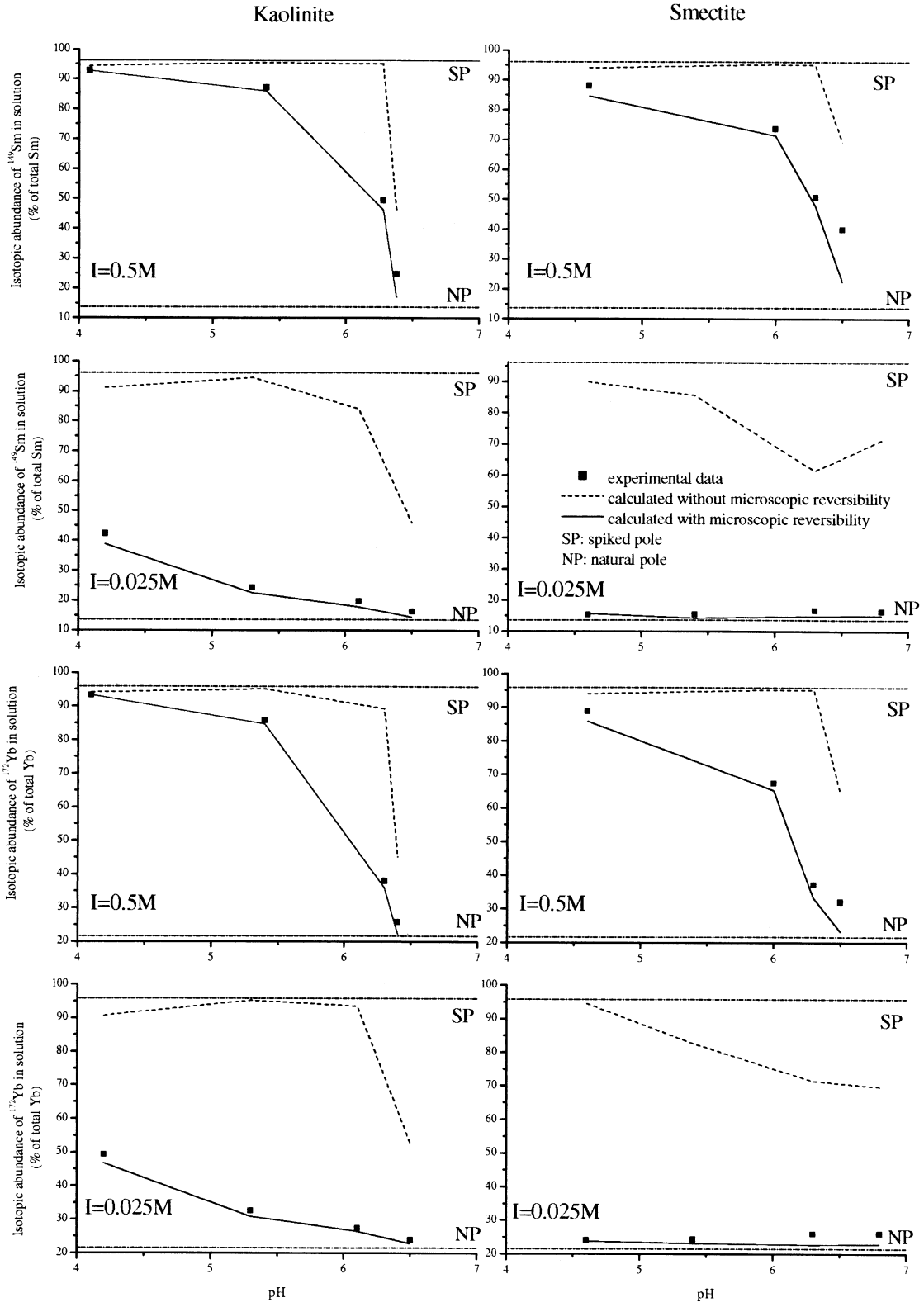

Fig. 5. ^{149}Sm and ^{172}Yb isotopic abundances in solution at the end of the experiments (355h), as a function of pH, for kaolinite and smectite at the two ionic strengths. Starting conditions: "Natural" solid and "Spiked" solution. Filled symbols (■): experimental data; dashed curve: isotopic abundances calculated with Eqn. 3; solid line: isotopic abundances calculated with Eqn. 4. The dashed-dotted lines indicate the isotopic compositions of the "Spiked" (SP) and the "Natural" (NP) end-members.

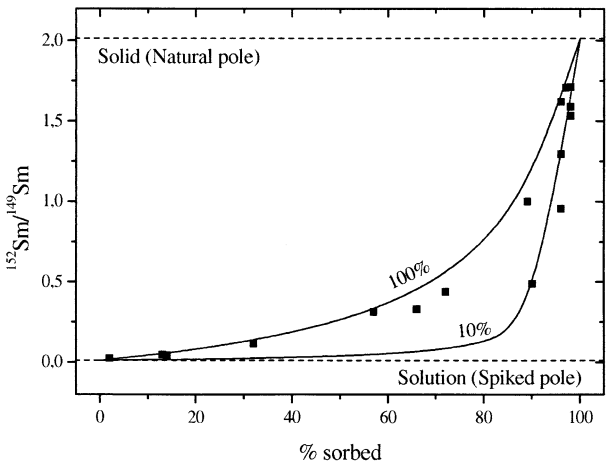

Fig. 6. $^{152}Sm/^{149}Sm$ ratio versus percentage of total lanthanide sorbed onto the solid, for the two clays at the two ionic strengths and 355 h of reaction time. Starting conditions: "Natural" solid and "Spiked" solution. Filled symbols (■): experimental data; solid lines: results obtained with Eqn. 2, for full equilibrium (100%), or partial exchange involving 10% of the lanthanides sorbed onto the solid (10%).

taken into account in these calculations. This implies that more sophisticated computations are required for a better understanding of the results, taking into account the two possible artefacts mentioned previously (see section 2.4.3) which are: (a) the presence, within the clay fraction, of an interstitial residual solution and (b) the release of REE from the solid in reaching chemical re-equilibrium. The effects of these two artefacts on the aqueous REE isotopic composition can be evaluated using the previous mixing equation (Eqn. 2), as we know the corresponding REE isotopic compositions and concentrations.

In the following equations, two boundary cases are considered:

(i) microscopic reversibility does not occur: that is, there is no exchange between the REE fraction sorbed onto the solid and the aqueous fraction;

(ii) the system reaches isotopic equilibrium: that is, it represents a dynamic equilibrium resulting from a continuous exchange between the atoms in the solid and in the solution.

In the first case, the isotopic composition of the REE in solution may change at the very beginning of the experiment due to the protocol artefacts mentioned above. After this rapid shift, the isotopic composition of the solution are assumed to remain stable throughout the reaction time, and solid and solution would remain in isotopic disequilibrium. In the second case, corresponding to a microscopic reversible process, the solid and the solution evolve towards the same isotopic composition intermediate between the two end-members.

Taking into account the artefacts, we can compute the isotopic compositions of the final solutions corresponding to the two boundary cases with the following equation:

$$A_{final}^{solution} = \frac{A_{initial}^{solution} N_{initial}^{solution} + A_{initial}^{solid} N_{residual}^{solution} + bA_{initial}^{solid}(N_{final}^{solution} - (N_{initial}^{solution} + N_{residual}^{solution}))}{N} \quad (3)$$

for a process with no microscopic reversibility and,

$$A_{final}^{solution} = \frac{A_{initial}^{solution} N_{initial}^{solution} + A_{initial}^{solid} N_{residual}^{solution} + A_{initial}^{solid} N_{initial}^{solid}}{N_{initial}^{solution} + N_{residual}^{solution} + N_{initial}^{solid}} \quad (4)$$

for a microscopic reversible equilibrium.

The parameters in these equations are defined as:

$A_{final}^{solution}$: abundance of the considered isotope in the final solution,

$A_{initial}^{solution}$: abundance of the considered isotope in the initial solution measured just before the inversion,

$N_{initial}^{solution}$: number of atoms of the considered element in the initial solution,

$A_{initial}^{solid}$: abundance of the considered isotope in the initial solid,

$N_{residual}^{solution}$: number of atoms of the considered element in the interstitial residual solution,

$N_{final}^{solution}$: number of atoms of the considered element in the final solution,

b and N: terms used to differentiate the two possible artefacts:

- $b = 0$ if $N_{final}^{solution} \leq N_{initial}^{solution} + N_{residual}^{solution}$
- $b = 1$ if $N_{final}^{solution} > N_{initial}^{solution} + N_{residual}^{solution}$
- $N = N_{initial}^{solution} + N_{residual}^{solution}$ if $b = 0$
- $N = N_{final}^{solution}$ if $b = 1$

$N_{initial}^{solid}$: number of atoms of the considered element in the initial solid.

Note that Eqn. 4 is a global mass balance equation in which the final abundance of a given isotope in the solution is identical to the value in the solid and the interstitial residual solution. This is independent of the process involved, such as the release or sorption of lanthanides by the solid.

Tables 3 and 4 report the isotopic compositions computed using these two equations, as a function of pH, while Figure 5 gives a comparison with the experimental data. In Figure 5, the dashed and the solid curves correspond to the results obtained with Eqn. 3 and 4, respectively. From these plots, it is evident that the results obtained from Eqn. 3 (no microscopic reversibility) are clearly different from the experimental data. This implies that the artefacts due to the experimental protocol cannot account for the measured final isotopic compositions. Clearly, the results obtained from Eqn. 4 are in better agreement with the measurements. However, the experimental data do not reproduce the computed simulations from Eqn. 4, particularly at high pH, where the difference between experimental and computed abundances can reach up to 17%. This discrepancy between experimental results and computed data is significant, leading us to conclude that part of the sorbed REE are not involved in the exchange process with aqueous REE.

The percentage of exchangeable sorbed cations can then be calculated as follows:

Table 5. Fraction of sorbed ^{149}Sm and ^{172}Yb affected by microscopic reversibility, as a function of pH. The uncertainties on % are calculated from analytical standard deviations.

	solution characteristics	Kaolinite I = 0.025 M				Kaolinite I = 0.5 M				Smectite I = 0.025M				Smectite I = 0.5M			
Natural Ln in solid and Spiked Ln in solution	pH (± 0.05)	4.17	5.25	6.12	6.48	4.08	5.40	6.27	6.44	4.57	5.40	6.31	6.77	4.64	5.95	6.34	6.47
	% of ^{149}Sm sorbed onto the solid affected by microscopic reversibility	83 (± 1)	83 (± 5)	71 (± 5)	48 (± 8)	100 (± 6)	86 (± 2)	85 (± 2)	29 (± 1)	100 (± 32)	58 (± 23)	44 (± 6)	53 (± 14)	65 (± 1)	87 (± 1)	87 (± 1)	25 (± 1)
	% of ^{172}Yb sorbed onto the solid affected by microscopic reversibility	85 (± 3)	82 (± 4)	82 (± 6)	50 (± 10)	97 (± 13)	88 (± 2)	85 (± 3)	28 (± 4)	90 (± 17)	58 (± 11)	30 (± 3)	23 (± 8)	65 (± 1)	88 (± 1)	71 (± 2)	16 (± 1)
Spiked Ln in solid and Natural Ln in solution	pH (± 0.05)	4.17	5.33	6.39	6.44	3.91	5.45	6.52	6.64	4.64	5.36	6.31	6.78	4.70	5.89	6.47	6.61
	% of ^{149}Sm sorbed onto the solid affected by microscopic reversibility	100 (± 2)	100 (± 4)	100 (± 2)	– –	88 (± 9)	90 (± 3)	79 (± 1)	45 (± 1)	50 (± 4)	17 (± 1)	9 (± 1)	25 (± 1)	100 (± 4)	98 (± 2)	76 (± 2)	34 (± 1)
	% of ^{172}Yb sorbed onto the solid affected by microscopic reversibility	100 (± 1)	100 (± 3)	85 (± 3)	60 (± 3)	81 (± 18)	100 (± 6)	75 (± 2)	35 (± 2)	100 (± 13)	67 (± 3)	16 (± 1)	17 (± 1)	100 (± 5)	100 (± 2)	62 (± 2)	23 (± 1)

$$E = \frac{(A^{solution}_{experimental} - A^{solution}_{initial})N^{solution}_{initial} + (A^{solution}_{experimental} - A^{solid}_{initial})N^{solution}_{residual}}{N^{solid}_{initial}(A^{solid}_{initial} - A^{solution}_{experimental})} * 100 \quad (5)$$

where:

E: exchangeable fraction in atoms (%),

$A^{solution}_{experiimental}$: abundance of the considered isotope measured in solution at the end of the experiment.

The other parameters are the same as in equations (3 and 4).

The results are reported in Table 5. As an example, Figure 7 presents the data obtained for ^{172}Yb in the case of smectite at low ionic strength as a function of pH. We observe a continuous decrease of the percentage of exchanged ^{172}Yb from low to high pH. From the data in Table 5**,** we can infer that, at pH $<$6.0, most of the atoms sorbed onto the solid participate in the microscopic reversibility process. On the contrary, at pH $>$6.5, just a small proportion of the atoms sorbed onto the solid participate in the microscopic reversibility process (see percentages in Table 5). An absence of full isotopic equilibration was also found in another experimental study based on the behaviour of ^{137}Cs in clay-water systems (Comans et al., 1991). These authors observed that the sorption of ^{137}Cs onto illite is only partially reversible. They attributed this phenomena to the slow migration of Cs to high-affinity sites (interlayers or frayed edges) from which this element is not easily released. Their measurements were performed at pH 7.8, which corresponds in the present study to the pH range where microscopic reversibility is incomplete. The role of pH can be interpreted in the light of surface speciation. Essentially, the negative permanent charge of the solid is compensated by physical sorption (outer-sphere complex formation) while chemical sorption (inner-sphere complex formation) occurs at the amphoteric sites (aluminol or silanol) on the edges of minerals. The physical sorption is pH-independent and predominates under acidic conditions. The chemical sorption is pH dependent and predominates in basic media. This interpretation is supported by recent results obtained by Time Resolved Laser Fluorescence Spectrometry (TRLFS) applied to the analysis of the sorption of Cm onto kaolinite and smectite at low ionic strength (Stumpf et al., 2001). In Figure 7, the computed percentages of exchanged REE in the solid are compared, as a function of pH, with the percentages of outer-sphere complexes derived from TRLFS by Stumpf et al. (2001) for Cm, in the case of smectite at low ionic strength. Although these two datasets concern different elements, the curves are strikingly similar.

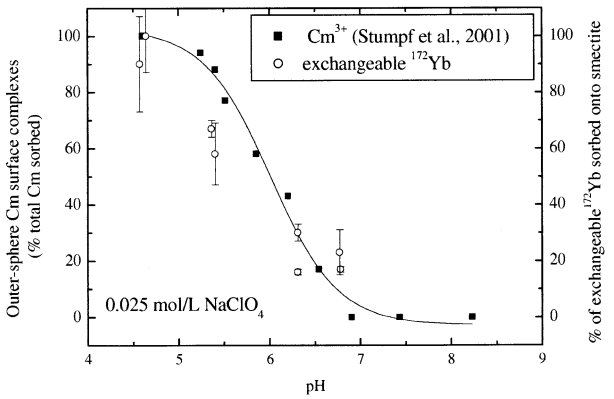

Fig. 7. Plot of pH versus percentage of Cm(III) adsorbed as outer-sphere complexes (data from Stumpf et al. 2001) as well as exchangeable ^{172}Yb sorbed onto the smectite at I=0.025 mol/L (the curve corresponds to a smoothed interpolation of literature data on Cm^{3+}(■)).

Thus, the results obtained in this study suggest that microscopic reversibility concerns mostly atoms sorbed as outer-sphere surface complexes. Moreover, inner-sphere complexes do not appear to contribute significantly—or not at all—to the microscopic reversibility process during the reaction time of our experiments. In principle, this is a realistic result since the chemical bonding for inner-sphere complexes is known to be significantly stronger than outer-sphere complexes.

5. CONCLUSION

We show that the microscopic reversibility of sorption for sorbed lanthanides onto smectite and kaolinite is not always complete. Reversibility is complete at acidic pH but incomplete at basic pH. We attribute the differences in the isotopic behaviour to the nature of the complexes formed at the clay surface. Atoms linked to the surface by physical sorption as outer-sphere complexes—predominant at low pH—appear easily exchangeable and the kinetics of the exchange reaction is very fast. By contrast, atoms linked to the surface by chemical sorption as inner-sphere complexes—predominant at high pH—are not easily exchangeable, at least at the time scale of our experiments, so the reaction must be very slow.

These results support the hypothesis that, under natural conditions, isotopic equilibrium between solutions and clays can be incomplete and disequilibrium may persist over long periods. These results can also help to better understand some experimental data on macroscopic irreversibility (Bonnot-Courtois and Jaffrezic-Renault, 1982). Another point of interest is the possibility to use the isotopic measurements to quantify the fraction of inner- and outer-sphere sorption as an alternative to the spectroscopic studies. This is suggested by the similarity between the values estimated in the present study and the values calculated from the TLRFS study. The quantification of each type of site will allow to test the models which link the apparent sorption properties with the sites density calculations.

Acknowledgments— This work is financially supported by the CNRS and ANDRA through the GdR FORPRO (Research action number 98.C) and corresponds to the GDR FORPRO contribution number 2001/24 A. We would also like to thank the technical staff for their valuable help: T. Aigouy, J. Escalier, R. Freydier and F. Ferrier. Dr M.S.N. Carpenter edited the English style. We are grateful to David R. Turner and Eric H. De Carlo, whose comments significantly improved this paper.

Associate editor: P. O'Day

REFERENCES

Aja S. U. (1998) The sorption of the rare earth element, Nd, onto kaolinite at 25°C. *Clays Clay Min.* **46,** 103–109.

Aries S., Valladon M., Polve M., and Dupre B. (2000) A routine method for oxide and hydroxide interference corrections in ICP-MS

chemical analysis of environmental and geological samples. *Geostand. News.: J. Geostand. Geoanal.* **24**(1), 19–31.

Bauer A. and Berger G. (1998) Kaolinite and smectite dissolution rate in high molar KOH solutions at 35 and 80°C. *Appl. Geochem.* **13,** 905–916.

Bauer A. and Velde B. (1999) Smectite transformation in high molar KOH solutions. *Clay Min.* **34,** 259–273.

Bonnot-Courtois C. and Jaffrezic-Renault N. (1982) Etude des échanges entre terres rares et cations interfoliaires de deux argiles. *Clay Minerals.* **17,** 409–420.

Comans R. N. J., Haller M., and Preter P. D. (1991) Sorption of cesium on illite: Non-equilibrium behaviour and reversibility. *Geochim. Cosmochim. Acta* **5,** 433–440.

Coppin F., Berger G., Bauer A., Castet S., and Loubet M. (2002) Sorption of lanthanides on smectite and kaolinite. *Chem. Geol.* **182,** 57–68.

Day P. R. (1965) Particle fractionation and particle size analysis. In *Methods of Soil Analysis* (ed. C. A. Black), pp. 545–567. Am. Soc. Agron. Inc.

De Carlo E. H., Wen X. Y., and Irving M. (1998) The influence of Redox Reactions on the uptake of dissolved Ce by Suspended Fe and Mn Oxide Particles. *Aqua. Geochim.* **3,** 357–389.

Goldstein S. J. and Jacobsen S. B. (1988) Rare earth elements in river waters. *Earth Planet. Sci. Lett.* **89,** 35–47.

Koeppenkastrop D. and De Carlo E. H. (1992) Sorption of rare-earth elements from seawater onto synthetic mineral particles: An experimental approach. *Chem. Geol.* **95,** 251–263.

Kosmulski M. (1997) Adsorption of Trivalent Cations on Silica. *J. Coll. Inter. Sci.* **195,** 395–403.

Kulik D. A., Aja S. U., Sinitsyn V. A., and Wood S. A. (2000) Acid-base surface chemistry and sorption of some lanthanides on K^+ Saturated Marblehead illite: II. A multisite-surface complexation modeling. *Geochim. Cosmochim. Acta* **64**(2), 195–213.

Laufer F., Yariv S., and Steinberg M. (1984) The adsorption of quadrivalent cerium by kaolinite. *Clay Min.* **19,** 137–149.

Marmier N., Dumonceau J., Chupeau J., and Fromage F. (1993) Etude comparée de la sorption des ions lanthanide trivalents sur la goethite et l'hématite. *Surf. Chem.* **317**(serie II), 1561–1567.

Maza-Rodriguez J., Olivera-Pastor P., Bruque S., and Jimenez-Lopez A. (1992) Exchange selectivity of lanthanide ions in montmorillonite. *Clay Min.* **27,** 81–89.

Meier L. P. and Kahr G. (1999) Determination of the cation exchange capacity (CEC) of clay minerals using the complexes of copper (II) ion with triethylenetetramine and tetraethylenepentamine. *Clays Clay Min.* **47**(3), 386–388.

Miller S. E., Heath G. R., and Gonzalez R. D. (1982) Effects of temperature on the sorption of lanthanides by montmorillonite. *Clays Clay Min.* **30**(2), 111–122.

Nagasaki S., Tanaka S., and Suzuki A. (1997) Affinity of finely disperserd montmorillonite colloidal particles for americium and lanthanides. *J. Nucl. Mat.* **244,** 29–35.

Sholkovitz E. R. (1995) The aquatic chemistry of rare earth elements in rivers and estuaries. *Aqua. Geochim.* **1,** 1–34.

Sholkovitz E. R., Elderfield H., Szymczak R., and Casey K. (1999) Island weathering: river sources of rare earth elemnts to the Western Pacific Ocean. *Mar. Chem.* **68,** 39–57.

Stumpf T., Bauer A., Coppin F., and Kim J. I. (2001) Time-Resolved Laser Fluorescence Spectroscopy. Study of the Sorption of Cm(III) onto Smectite and Kaolinite. *Env. Sci. Tech.* **35,** 3691–3694.

Turner D. R., Pabalan R. T., and Beretti F. P. (1998) Neptunium (V) sorption on montmorillonite: An experimental an surface complexation modeling study. *Clays Clay Min.* **46**(3), 256–269.

Undabeytia T., Nir S., Rytwo G., Morillo E., and Maqueda C. (1998) Modeling adsorption-desorption processes of Cd on montmorillonite. *Clays Clay Min.* **46,** 423–428.

Wang X., Dong W., Dai X., Wang A., Du J., and Tao Z. (2000) Sorption and desorption of Eu and Yb on alumina: mechanisms and effect of fulvic acid. *Appl. Rad. Iso.* **52,** 165–173.